Biochimie 154 (2018) 176–186

Contents lists available at ScienceDirect

Biochimie

journal homepage: www.elsevier.com/locate/biochi

Research paper

Elucidating paramylon and other carbohydrate metabolism in *Euglena gracilis*: Kinetic characterization, structure and cellular localization of UDP-glucose pyrophosphorylase

Robertino J. Muchut [a, b], Rodrigo D. Calloni [a, b], Fernando E. Herrera [b], Sergio A. Garay [b], Diego G. Arias [a, b], Alberto A. Iglesias [a, b], Sergio A. Guerrero [a, b, *]

[a] Laboratorio de Enzimología Molecular, Instituto de Agrobiotecnología del Litoral (CONICET - UNL), Argentina
[b] Facultad de Bioquímica y Ciencias Biológicas, Universidad Nacional del Litoral, Argentina

ARTICLE INFO

Article history:
Received 18 July 2018
Accepted 12 September 2018
Available online 15 September 2018

Keywords:
UDP-Glucose
Uridylyltranferase
Carbon storage
β-1,3-Glucan
Euglena gracilis

ABSTRACT

Many oligo and polysaccharides (including paramylon) are critical in the *Euglena gracilis* life-cycle and they are synthesized by glycosyl transferases using UDP-glucose as a substrate. Herein, we report the molecular cloning of a gene putatively coding for a UDP-glucose pyrophosphorylase (*Egr*UDP-GlcPPase) in *E. gracilis*. After heterologous expression of the gene in *Escherichia coli*, the recombinant enzyme was characterized structural and functionally. Highly purified *Egr*UDP-GlcPPase exhibited a monomeric structure, able to catalyze synthesis of UDP-glucose with a V_{max} of 3350 U.mg^{-1}. Glucose-1P and UTP were the preferred substrates, although the enzyme also used (with lower catalytic efficiency) TTP, galactose-1P and mannose-1P. Oxidation by hydrogen peroxide inactivated the enzyme, an effect reversed by reduction with dithiothreitol or thioredoxin. The redox process would involve sulfenic acid formation, since no pair of the 7 cysteine residues is close enough in the 3D structure of the protein to form a disulfide bridge. Electrophoresis studies suggest that, after oxidation, the enzyme arranges in many enzymatically inactive structural conformations; which were also detected *in vivo*. Finally, confocal fluorescence microscopy provided evidence for a cytosolic (mainly in the flagellum) localization of the enzyme.

1. Introduction

The evolutionary process that led to the appearance of plant-like photosynthetic eukaryotes began with the endosymbiotic uptake of a cyanobacterium by a heterotrophic eukaryote. From this are derived the so-called primary plastids found in algae (green and red) and in higher plants [1,2]. In this process, algae, some protozoa and diatoms occupy a position of relevance. Besides, diatoms and euglenoids are products of a secondary endosymbiosis, where a photosynthetic eukaryotic cell was phagocytized by a heterotrophic eukaryote [3]. These events during evolution gave rise to different types of organisms, with important differences with respect to cellular structure and metabolic function. Biochemically, there are found different groups of organisms that accumulate reserve polysaccharides in the form of α-1,4-polyglucans (linear or with α-1,6 branches related to glycogen, phytoglycogen and starch) or β-1,3-glucans (linear or with β-1,6 branches, mainly the paramylon or crysolaminarin polymer, respectively) [2].

Euglenoids are flagellate organisms belonging to the protist phylum Euglenozoa, which also includes kinetoplastids (bodonids and trypanosomatids), diplonemids, and the most recently characterized symbiontids [4,5]. The particular grouping of such diverse organisms within the Euglenozoa phylum, mainly non-photosynthetic eukaryotes, is based on clear morphological similarities, conserved molecular traits and phylogenetic analyzes. For example, all euglenoids added a splicing leader to almost all mRNAs encoded in the nucleus, by a spliceosome-dependent *trans*-splicing mechanism [6,7]. In addition, Euglenozoa is included within the group Excavata, along with other parasites like *Giardia* spp. (Fornicata) [8,9] and *Trichomonas* spp. (Parabasalia) [10], being

* Corresponding author. Instituto de Agrobiotecnología del Litoral (IAL), CCT-CONICET Santa Fe, Colectora Ruta Nac. Nº 168 km 0 - Paraje El Pozo (3000), Santa Fe, Argentina.
E-mail addresses: saguerrero@santafe-conicet.gov.ar, sguerrer@fbcb.unl.edu.ar (S.A. Guerrero).

https://doi.org/10.1016/j.biochi.2018.09.006
0300-9084/

Abbreviations

DTT	Dithiothreitol
Man-1P	Mannose-1-phosphate
Gal-1P	Galactose-1-phosphate
Glc-1P	Glucose-1-phosphate
GlcN-1P	Glucosamine-1-phosphate
GalN-1P	Galactosamine-1-phosphate
GlcNAc-1P	N-acetylglucosamine-1-phosphate
IAM	Iodoacetamide
UDP-Glc	UDP-glucose
UDP-GlcPPase	UDP-glucose pyrophosphorylase

considered as the most basal eukaryotic branch [11].

Euglena gracilis is a microorganism capable of performing photosynthesis or growth in the dark, when a carbon source is available in the medium. Very valuable information about genes coding for enzymes belonging to the *E. gracilis* metabolism emerged from recent works on transcriptome analysis [12,13]. In one way or another, this organism accumulates different bioactive compounds; in particular the polysaccharide paramylon [14–16] and the wax ester myristyl myristate, the two main sources of energy reserve in this protist [17]. The storage polysaccharide paramylon is located in the cytosol as crystalline granules and is composed of β-1,3-linked glucose units, unlike α-1,4-glucans found in plants, animals and bacteria. Paramylon is synthesized by the transfer of a glucose moiety from UDP-Glc to its non-reducing extreme in a reaction catalyzed by a paramylon synthase (Fig. 1).

UDP-GlcPPase (UTP:α-D-glucose uridylyltransferase, EC 2.7.7.9) plays a relevant role for paramylon synthesis and other sugar metabolic pathways in *E. gracilis* (Fig. 1). The enzyme catalyzes the production of UDP-Glc, in presence of Mg^{2+}, according to the reaction: Glc-1P + UTP ↔ UDP-Glc + PPi. This enzyme was previously identified and characterized in other organisms [18–21]. Based on analysis of transcriptomic data from *E. gracilis* [12,13], we identified a gene coding for a putative *Egr*UDP-GlcPPase. Herein, we report the molecular cloning of the gene, followed by the production and purification of the recombinant enzyme. The pure enzyme was kinetically characterized and studied with respect to its sensitivity to changes in the redox environment. We also present results from assays of subcellular localization determined by means of specific antibodies and confocal fluorescence microscopy.

2. Materials and methods

2.1. Chemicals

Glc-1P, Gal-1P, GlcN-1P, GalN-1P, GlcNAc-1P, Man-1P, UTP, TTP, CTP, GTP, ATP, diamide, DTT, IAM, protein standards and IPTG were obtained from Sigma-Aldrich. All other reagents were of the highest quality available.

2.2. Bacteria and plasmids

Escherichia coli Top 10 F′ (Invitrogen) cells were used for cloning purposes. Gene was expressed using pET28c (Novagen) vector and *E. coli* BL21 (DE3) (Invitrogen) cells as host. DNA manipulations and *E. coli* cultures as well as transformations were performed according to standard protocols [22].

2.3. E. gracilis cultivation

E. gracilis UTEX 753 cells were grown in T flask or erlenmeyers in static conditions. Cells were grown autotrophically with 16/8 h light/dark cycle, in Cramer & Myers medium (C&M) [23], at a temperature of 22–24 °C with luminous intensity of 60 μmol photons.m^{-2}.s^{-1}. Or in heterotrophic conditions, cells grew static

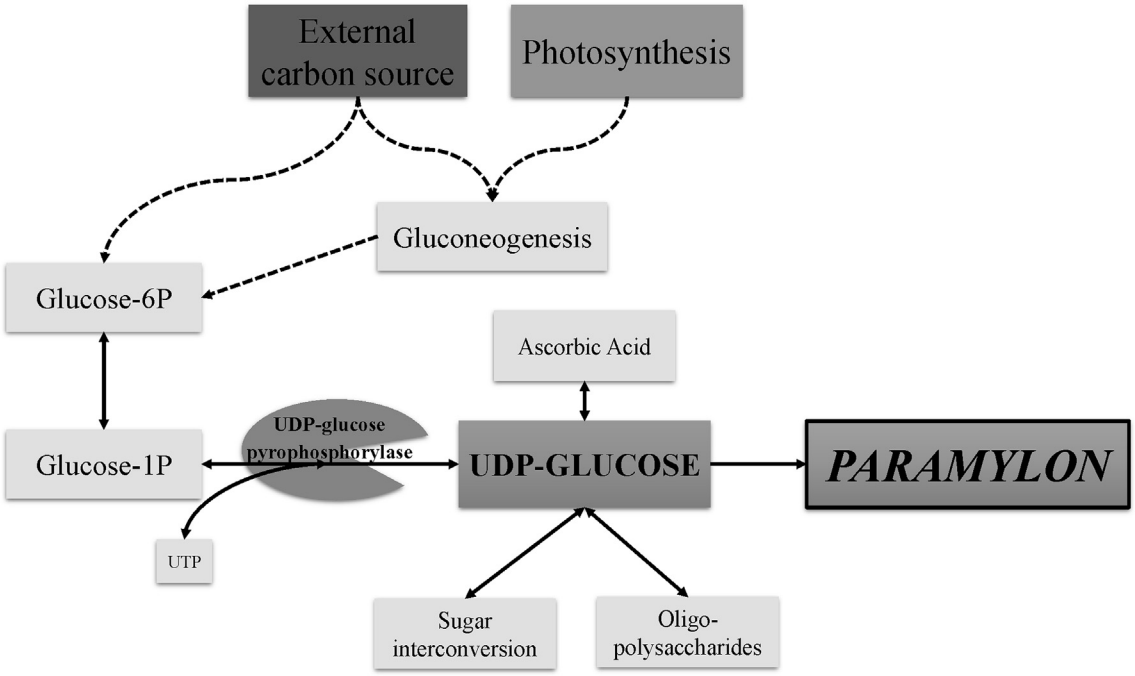

Fig. 1. Simplified scheme of carbon utilization flow in *Euglena gracilis*. UDP-glucose pyrophosphorylase catalyzes the synthesis of UDP-glucose, a key metabolite in carbohydrate metabolic pathways.

in the dark at a temperature of 28 °C in C&M medium supplemented with 1% glucose. To achieve anaerobiosis, T flasks or erlenmeyers were completely filled with medium avoiding the presence of air.

2.4. Cloning of UDP-GlcPPase gene from E. gracilis

The gene (*egrgalU*) coding for UDP-GlcPPase from *E. gracilis* was designed for *de novo* synthesis (BIO BASIC INC) according to transcriptome information (light_m10179) from *E. gracilis* [12], in (http://jicbio.nbi.ac.uk/euglena), using codon optimization for heterologous expression in *E. coli* cells. The constructed gene was flanked by *Nde*I and *Hind*III restriction sites for afterwards cloning and expression in *E. coli* cells. The pUC57 plasmids harboring the *egrgalU* gene was digested with *Nde*I and *Hind*III. Released gene was defined electrophoretically in 1% (w/v) agarose gel and purified using a Wizard SV gel & PCR Clean Up kit (Promega). The digested gene was subcloned into pET28c to obtain the construct [pET28c/*egrgalU*] including an N-terminal His-tag. This construct was used to transform *E. coli* BL21 (DE3) competent cells.

2.5. Protein expression and purification

E. coli BL21 (DE3) cells transformed with [pET28c/*egrgalU*] were grown at 37 °C in LB medium supplemented with 50 μg.ml^{-1} kanamycin until reach an OD_{600} ~ 0.6. Protein expression was induced with 0.4 mM IPTG at 25 °C for 16 h. Cells were harvested by centrifuging 15 min at 4 °C and 5000 × *g*, and the pellet suspended in 5 ml of buffer A [25 mM Tris−HCl pH 8.0, 300 mM NaCl, 5% (v/v) glycerol, 10 mM imidazole] per g of cells. Cells were disrupted by sonication on ice and centrifuged at 16,000 × *g* for 20 min at 4 °C. *Egr*UDP-GlcPPase was purified by ion metal affinity chromatography (IMAC), using 1 ml HisTrap™ HP columns (GE Healthcare). Briefly, supernatants were loaded onto previously equilibrated Ni^{2+} charged columns. After extensively washing with buffer A, samples were eluted with a 10−300 mM imidazole lineal gradient (50 column volumes). Active fractions were pooled, dialyzed to eliminated imidazole and supplemented with 10% (v/v) glycerol. All proteins were stable for at least three months when stored at −80 °C under these conditions.

2.6. Protein methods

Protein concentration was determined by the Bradford procedure [24] using bovine serum albumin as a standard. Proteins were defined electrophoretically in SDS-PAGE (in presence or absence of reducing agent) according to Laemmli [25] [polyacrylamide monomer concentration was 10% (w/v) for the separating gel and 4% (w/v) for the stacking gel], or in native PAGE (in the absence of SDS) [26]. For native PAGE, the final polyacrylamide monomer concentration was 7% (w/v). Coomassie Brilliant Blue was used for protein staining.

E. gracilis protein extract was prepared suspending cells in lysis buffer (50 mM MOPS-NaOH pH 8.0, 1 mM EDTA (plus a cocktail of protease inhibitors) and disrupted by sonication on ice (2 s pulse on with intervals of 4 s pulse off for a total time of 2 min). Proteins in SDS-PAGE or native PAGE were blotted onto a nitrocellulose membrane. The membrane was blocked overnight at 4 °C with 5% skimmed milk in PBS (8 g.l^{-1} NaCl, 0.2 g.l^{-1} KCl, 1.44 g.l^{-1} Na_2HPO_4, 0.24 g.l^{-1} KH_2PO_4, pH 7.4), subsequently incubated with primary antibody at room temperature for 1 h, and then incubated with a HRP-conjugated anti-rabbit secondary antibody for 1 h. Bands were visualized using the ECL Western blotting detections reagents (Thermo Scientific). Serum anti-*Egr*UDPGlcPPase was prepared by rabbit immunization [27].

For fraction analysis of *Egr*UDP-GlcPPase, *E. gracilis* cells were disrupted by sonication as previously described. Then, the lysate was centrifuged for 60 min at 14,000 × *g* at 4 °C. The soluble fraction was treated with 8 mM $CaCl_2$ (for vesicle and microsome precipitation) and insoluble fraction was treated with 100 mM Na_2CO_3, pH 11.0 (for solubilization of protein associated to membrane). After incubation for 30 min at 4 °C, the samples were centrifuged for 30 min at 14,000 × *g* [28]. Soluble and insoluble fractions obtained in both procedures were analyzed by western blot, using specific polyclonal sera against *Egr*UDP-GlcPPase (diluted 1/1000).

The analysis of the enzyme structure under oxidative or alkylation conditions were performed by means of native PAGE and/or SDS-PAGE (with or without reducing agent). DTNB (5,5′-dithiobis-2-nitrobenzoic acid) was used for the quantification of free thiols in the pure recombinant protein treated with diamide, H_2O_2, IAM, DTT or in the absence of any agents as described previously [29].

2.7. Molecular mass determination

To determine the quaternary structure of *Egr*UDP-GlcPPase, the purified enzyme was subjected to gel filtration chromatography. Sample was loaded in a Superdex Tricorn 10/300 column (GE Healthcare) in buffer G (50 mM HEPES−NaOH pH 8.0, 100 mM NaCl, and 0.1 mM EDTA). The molecular mass was calculated using a calibration plot constructed with protein standards from GE Healthcare, including thyroglobulin (669 kDa), ferritin (440 kDa), aldolase (158 kDa), conalbumin (75 kDa), ovalbumin (44 kDa), carbonic anhydrase (29 kDa), ribonuclease A (13.7 kDa) and aprotinin (6.5 kDa). The column void volume was measured using a dextran blue loading solution (Promega). To determine the effect of oxidation in the quaternary structure of *Egr*UDP-GlcPPase, the enzyme was incubated 30 min (25 °C) with 5 mM diamide. After treatment the samples were analyzed by gel filtration.

2.8. Enzyme assay

*Egr*UDP-GlcPPase activity was assayed in the UDP-Glc synthesis direction measuring inorganic phosphate (Pi) released after hydrolysis of pyrophosphate (PPi) by using a highly sensitive colorimetric method [30]. Standard reaction mixtures contained 50 mM MOPS-NaOH (pH 8.0), 10 mM $MgCl_2$, 1.5 mM UTP, 0.2 mg.ml^{-1} bovine serum albumin, 0.5 mU.μl^{-1} yeast inorganic pyrophosphatase and a proper enzyme dilution. Assays were initiated by addition of 1.5 mM Glc-1P in a final volume of 50 μl. Reaction mixtures were incubated for 10 min at 37 °C and terminated by adding Malachite Green reactive. The complex formed with the released Pi was measured at 630 nm with an ELISA Microplate Photometer Multiskan Ascent (Thermo Scientific). Controls were made to ensure the measurement of initial velocity (v_o), that is the rate where product formation was practically linear with time and the total consumption of substrates was below 10%. One unit (U) of enzyme activity is equal to 1 μmol of product (PPi) formed per minute under the respective assay conditions specified above. The same procedure was followed for the analysis of enzyme promiscuity towards other sugar-1P or nucleoside triphosphate.

2.9. Calculation of kinetic constants

Kinetic assays were performed using specified concentrations and conditions for all reaction mixture components. Saturation curves were performed by assaying the respective enzyme activity at saturating level of a fixed substrate and different concentrations of the variable substrate. The experimental data were plotted as

enzyme activity ($U.mg^{-1}$) versus substrate concentration (mM), and kinetic constants were determined by fitting the data to the modified Hill equation: $v_o = V_{max}[S]^n/(S^n_{0.5} + [S]^n)$. All kinetic constants are the mean of at least three sets of data, which were reproducible within ±10%.

2.10. Oxidation, alkylation and reduction assays

Oxidation or alkylation of cysteine residues was carried out by incubating the enzyme (7 μM) at 25 °C in buffer A with different concentrations of either diamide, H_2O_2, oxidized glutathione (GSSG), S-nitrosocysteine (CysNO) or iodoacetamide (IAM). Aliquots were taken at different incubation times, diluted and assayed for activity (see 2.8 section). Experimental data were plotted as remaining activity versus oxidation time (min) or versus reagent concentration. For calculation of percentage of remaining activity, 100% was considered as the activity when the enzyme was incubated under the same conditions but in the absence of oxidant or alkylant. Experimental points determined in redox modification studies are means of at least three measurements reproducible within ±10%.

To remove any reagent excess, the enzyme (as specified above) was diluted to final factor of 100,000 or desalted using Bio-Gel P6 (Bio-Rad) desalting mini column.

2.11. Molecular modeling

The search for suitable template models was made with the template identification tool of the Swiss Model Workspace [31]. Deduced crystal structure model of UDP-GlcPPase from *Leishmania major* (PDB ID 4m2a) that showed the best homology to *Egr*UDP-GlcPPase (54% identity) [32] was used as template for homology modeling. Sequences of the selected template were aligned using the program HHBlits [33] and 10 homology models of *Egr*UDP-GlcPPase were obtained using the software Modeller 9.15 [34,35]. Special care was taken to avoid any gap inside of secondary structure elements. The best model was established taken into account the higher global score of verify3D [36], the higher z-DOPE [37] and the QMEAN [38] potential values.

2.12. Immunolocalization by confocal microscopy

E. gracilis cells obtained from autotrophic or heterotrophic cultures were washed twice for 15 min at room temperature in PBS and fixed in 4% (v/v) formaldehyde. After washing they were permeabilized and blocked during 4 h in a medium containing PBS supplemented with 0.1% (v/v) Tween 20 and 3% (w/v) BSA. Fixed samples were incubated first with specific polyclonal antibodies (1/100 dilution) and thereafter with Cy3 conjugated goat anti-rabbit antibody (1/500 dilution). Incubation with the primary and secondary antibodies was performed at 4 °C during 6 h. After washing, the slides were finally mounted with antifade mounting solution and visualized under a confocal microscope (Leica TCS SP8).

3. Results

3.1. Expression and properties of recombinant EgrUDP-GlcPPase

The identification of a nucleotide sequence (see 2.4) coding for a putative UTP:Glc-1P uridylyltransferase from *E. gracilis* [12], led us to perform the *de novo* synthesis of the full-length gene (*egrgalU*). This 1380 bp gene is predicted to encode a 459 amino acid protein (*Egr*UDP-GlcPPase) with a calculated pI of 5.2. To explore the protein functionality, the synthesized gene was cloned into the prokaryotic expression vector pET28c. The expression in *E. coli* BL21 (DE3) produced a recombinant protein as a polypeptide fused to a His-tag at the N-terminus. The soluble fraction was chromatographically purified on a Ni^{2+} affinity resin, to obtain the protein with purity higher than 98%, as judged by SDS-PAGE analysis (Fig. 2A, lane 2). The molecular mass revealed for the protein agrees with the expected size (49.7 kDa) deduced from its amino acid sequence, and it is similar to those from other UDP-GlcPPases found in eukaryotes [18,21,39,40]. The quaternary structure of the pure protein was analyzed by size exclusion chromatography. *Egr*UDP-GlcPPase eluted as a single peak with a retention volume compatible with a monomeric structure (Fig. 3A), which is in agreement with previous reports for the enzyme from *L. major* [41] and *Giardia lamblia* [18].

*Egr*UDP-GlcPPase exhibited a strict requirement of $MgCl_2$ for catalytic activity. Table 1 shows the kinetic properties of the

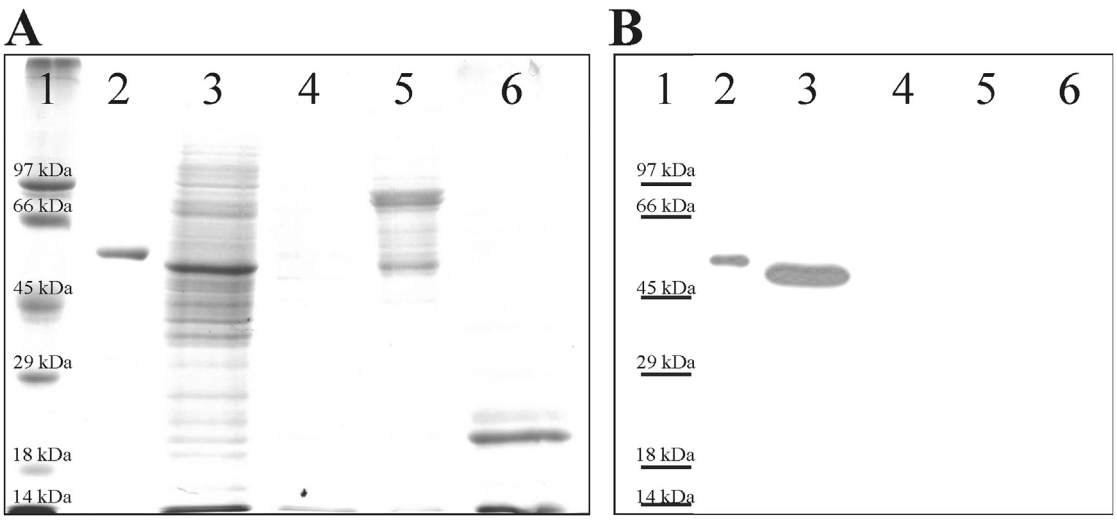

Fig. 2. Electrophoretic analysis of soluble and membranous fractions from *E. gracilis*. **A.** SDS-PAGE stained with Coomassie blue. **B.** Western-blotting of gel A revealed with sera anti-*Egr*UDP-GlcPPase. Lane **1,** molecular mass markers. Lane **2,** purified recombinant *Egr*UDP-GlcPPase (0.5 μg in **A** and 1 ng in **B**). Lane **3,** soluble fraction from treatment with $CaCl_2$. Lane **4,** insoluble fraction from treatment with 8 mM $CaCl_2$. Lane **5,** soluble fraction from treatment with 100 mM $NaCO_3$ pH 11.0. Lane **6,** insoluble fraction from treatment with 100 mM $NaCO_3$ pH 11.0. Further details of the different treatments are detailed in section 2.6.

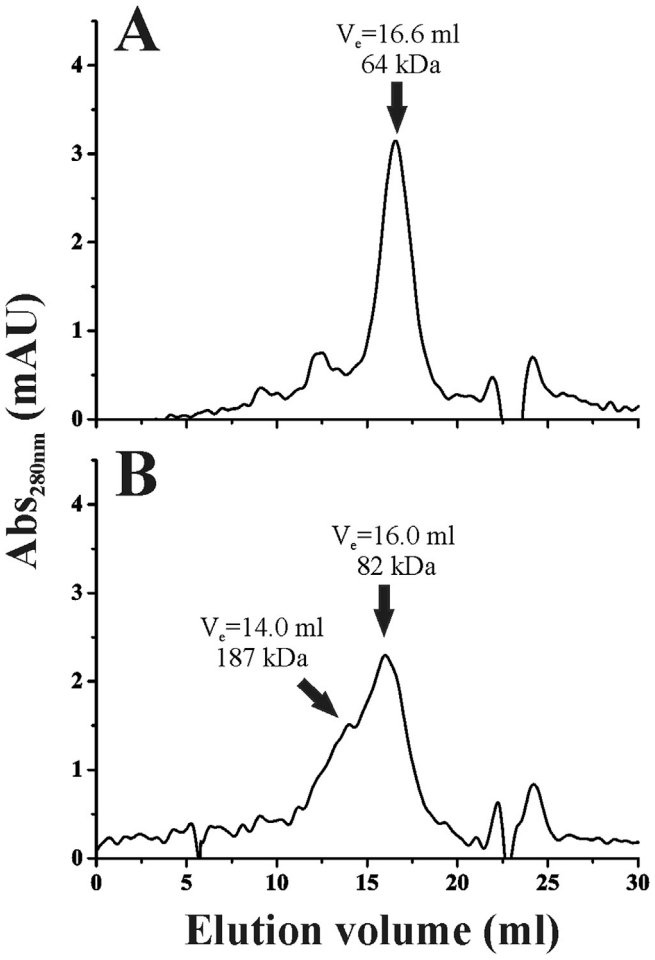

Fig. 3. Size exclusion chromatography profiles of *Egr*UDP-GlcPPase. **A.** The purified enzyme mainly eluting as a monomer of 64 kDa. **B.** The enzyme after incubation for 30 min with diamide, showing a wider elution profile with forms of different molecular size and possible formation of oligomers.

enzyme with respect to the use of UTP and Glc-1P or alternative substrates. Compared to homologous enzymes from other organisms, *Egr*UDP-GlcPPase exhibited a relatively high V_{max} and comparable affinity for UTP and Glc-1P [18,20,41–43]. The recombinant enzyme was unable to utilize ATP, CTP, GTP, GlcN-1P, GalN-1P, or GlcNAc-1P (assayed up to 2 mM). However, it used as alternative substrates TTP (to synthesize TDP-Glc), Gal-1P and Man-1P (both sugar-1Ps analyzed in combination with UTP) (Table 1); as previously found for the enzyme from *Xanthomonas* spp [42]. (respect to TDP-Glc) and *G. lamblia* [18] (producing TDP-Glc and UDP-Gal). The enzyme exhibited slightly cooperative saturation curves for TTP and Gal-1P, with similar apparent affinity but reaching a lower V_{max} compared with the use of UTP or Glc-1P. Consequently, the catalytic efficiency (calculated as $k_{cat}/S_{0.5}$, analogous to k_{cat}/K_m for hyperbolic kinetics [44]) of the *Egr*UDP-GlcPPase for synthesis of TDP-Glc or UDP-Gal was 25-fold lower than for producing UDP-Glc. Concerning the use of Man-1P, kinetics displayed a quite unusual behavior, since no saturation conditions could be reached (even at 10 mM Man-1P). We estimated approximate values of V_{max} and $S_{0.5}$ (Table 1), denoting catalytic efficiencies of the enzyme using these alternative substrates that were two orders of magnitude lower compared to the value obtained for Glc-1P.

Table 1
Kinetics parameters of *Egr*UDP-GlcPPase.

	$S_{0,5}$ (mM)	n_H	k_{cat} (s^{-1})	$k_{cat}/S_{0.5}$ ($M^{-1}s^{-1}$)
Glc-1P	0.24 ± 0.01	1.01 ± 0.03	2792	116.3×10^5
UTP	0.172 ± 0.004	1.16 ± 0.03		162.3×10^5
TTP	0.28 ± 0.01	1.40 ± 0.09	192	6.8×10^5
Gal-1P	0.80 ± 0.02	1.49 ± 0.04	263	3.3×10^5
Man-1P	>4	n.d.	169[a]	$<0.4 \times 10^5$

n.d., not determined.
[a] From apparent velocity reached at 10 mM Man-1P.

In our hands, the recombinant *Egr*UDP-GlcPPase was insensitive to regulation by allosteric effectors. So far, we analyzed that the activity of the enzyme was not affected by different metabolites (i.e., Fru-6P, Glc-6P, 3P-glycerate, Fru-1,6-bisP, AMP, and Pi) that are key intermediates of central metabolic pathways for carbon and energy in photosynthetic organisms (many of these compounds are effectors of ADP-GlcPPase [45,46]).

3.2. *EgrUDP-GlcPPase is located in cytosol*

With the purpose of determining if the enzyme localizes in the cytosol or is associated with any of the cellular membrane systems, we grew *E. gracilis* to perform two assays. First, after cellular disruption, the soluble fraction was added with 8 mM $CaCl_2$ to precipitate microsomal membranes [47]. Lane 3, in Fig. 2B, shows a recognition signal in the soluble fraction (not precipitated with $CaCl_2$). On the other hand, the membranous fraction obtained by centrifugation after cell disruption was treated with 100 mM Na_2CO_3 pH 11.0 to analyze if the enzyme could be associated with plasmatic membrane. The lack of recognition signal by the antibody shown in Fig. 2B (lanes 4, 5 and 6), argues against a location of the enzyme associated with membranes.

E. gracilis cells from autotrophic and heterotrophic cultures were also used to search for the cellular localization of *Egr*UDP-GlcPPase by means of confocal microscopy. Interestingly, we detected a recognition signal in the cytosol, stronger at the flagellar region (Fig. 4). The enzyme was not associated either with microsomes or membranes, in agreement with results shown in Fig. 2. The immunolocalization carried out using a secondary Cy3-conjugated goat anti-rabbit antibody allowed us to discriminate fluorescence produced by chlorophyll. Using a 552 nm laser we excited both the Cy3 dye and the chlorophyll but, since the fluorescence emission wavelength of chlorophyll is greater than that emitted by the Cy3 dye, we could easily discriminate them. The high signal detected at flagella agrees with previous work [48] where Chen and Bouck characterized the occurrence of endogenous glycosyl transferases in flagella of *E. gracilis* strain Z. This supports the presence of an increased concentration of the enzyme providing UDP-Glc for the synthesis of glycoproteins, glycolipids and oligosaccharides.

3.3. *EgrUDP-GlcPPase activity is redox modulated*

Based on previous reports about modification by redox thiol-disulfide bond exchange mechanism affecting the activity of UDP-GlcPPases from *Giardia lamblia* and *Entamoeba histolytica* [18,20], we evaluated the potential effect of thiol-reactive agents on *Egr*UDP-GlcPPase. In a first approach, the treatment of the enzyme with H_2O_2 or diamide caused a time dependent inhibition of the enzyme, to reach ~40% of remaining activity after 30 min (Fig. 5A). This inhibitory effect was observed with others oxidant reagents, such as GSSG or CysNO (Fig. 5B). Interesting, iodoacetamide (IAM), a thiol blocker reagent, exhibited similar inhibitory effect on the enzyme (Fig. 5B).

We also performed chemical determination of thiol groups in the enzyme using the reagent DTNB [29,49]. We quantified seven thiol groups form per polypeptide in the purified *Egr*UDP-GlcPPase (Table 2), which is in agreement with the number of Cys residues

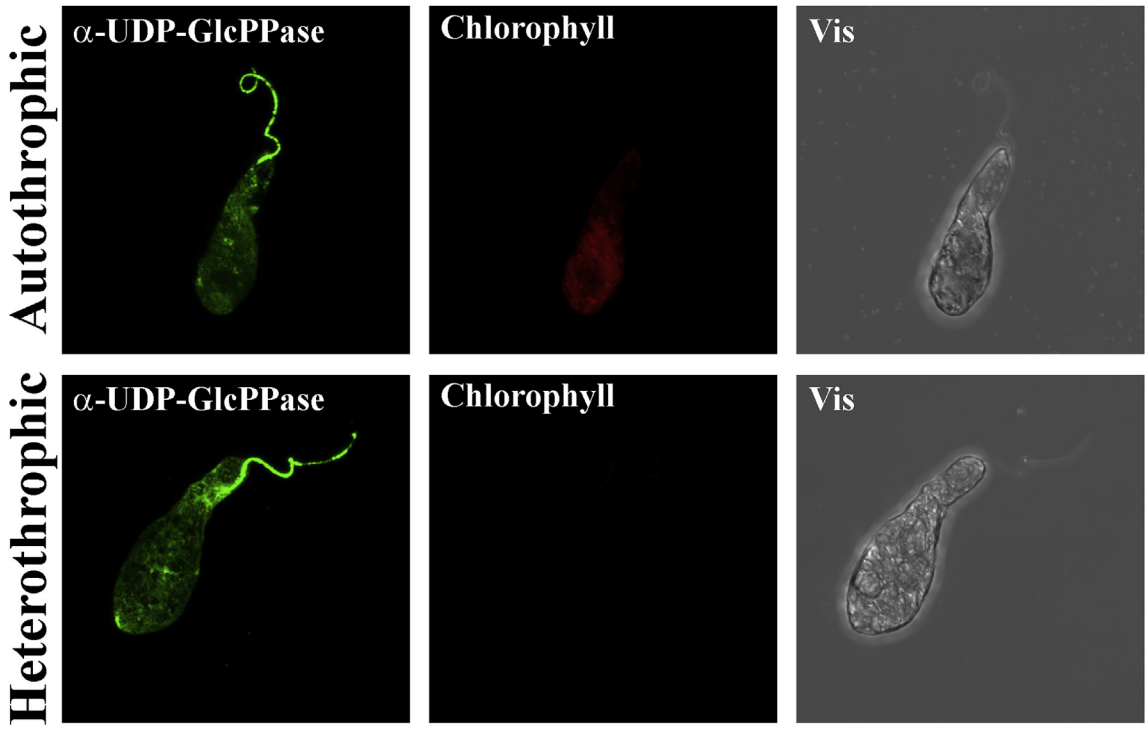

Fig. 4. Maximum projection of confocal microscopy image of *E. gracilis* cells growth autotrophically in C&M medium and heterotrophically in C&M medium supplemented with Glc 1% (w/v). Both were treated with primary antibody anti-*Egr*UDP-GlcPPase and secondary antibody anti-rabbit conjugated to Cy3 (α-UDP-GlcPPase, green). Chlorophyll fluorescence (Chlorophyll, red). Transmitted light (Vis, gray).

found in the primary structure of the enzyme. After extreme treatment with H_2O_2, diamide or IAM only two thiols remained detected, suggesting the oxidation of five Cys residues per mol of enzyme. On the other hand, an analysis by non-reducing SDS-PAGE of the different redox forms of *Egr*UDP-GlcPPase revealed that the enzyme treated with H_2O_2 or diamide migrated slightly faster (Fig. 5B). This dissimilar apparent size of the enzyme indicates that oxidation of the enzyme could involve the formation of intramolecular (but not intermolecular) disulfide bonds after oxidation, as the covalent crosslink between Cys residues within the polypeptide could lead to a more compact structure [18,20], modifying the Stokes radius and consequently changing the electrophoretic motility. On the contrary, treatment with GSSG, CysNO or IAM did not change the migration profile. Interestingly, the inhibitory effect of the oxidizing agents could be reversed by incubation with 5 mM DTT or reduced thioredoxin (Fig. 5C), which returned the enzyme from its low activity state to a fully active condition. All these results indicate that thiol groups in critical Cys residues are important for the functionality of the enzyme, with oxidation or alkylation of such residues provoking a loss of the activity. Interestingly, the cellular presence of redox effectors (such as H_2O_2, GSSG, CysNO and thioredoxin) supports that the enzyme would be redox-modified and its activity modulated *in vivo*.

3.4. *EgrUDP-GlcPPase adopts different conformations after redox modification, in vitro as well as in vivo*

Analysis by size exclusion chromatography of *Egr*UDP-GlcPPase showed changes in the elution profile of the oxidized protein. The recombinant enzyme eluted in a single peak as monomer (~65 kDa), but when was treated with diamide showed the presence of species with higher apparent molecular mass than the monomer (~80—~190 kDa) (Fig. 3B). The treatment with DTT of the oxidized enzyme produced a recovery not only of activity but also of its monomeric structure (data no-shown). Fig. 6 shows a 3D structure of the enzyme developed by molecular modeling using the crystalyzed UDP-GlcPPase from *L. major* as the template. A fact arising from the molecular model is that none of the seven Cys residues is close enough to another to eventually form an intramolecular disulfide bond. This result argues against the hypothesis that the oxidation process in *Egr*UDP-GlcPPase takes place via the formation of intramolecular disulfides, as is the case for the homologous enzyme from other protozoa [18,20]. It can be assumed that oxidation of sulfhydryl residues (perhaps randomly from the five reactive cysteines) in *Egr*UDP-GlcPPase leads to the formation of sulfenic acid derivatives. The latter groups add negative charges to the protein structure, thus changing charge:mass ratio and/or inducing localized conformational changes. Also, Cys sulfenic acid in proteins was found able to be reduced again to Cys by DTT and other reductants [50], as we observed in the *E. gracilis* enzyme.

Closely related to results from size exclusion chromatography, we found that in the presence of increasing concentrations of both H_2O_2 (from 0 to 14 mM) and IAM (from 0 to 7 mM), the purified enzyme analyzed in a native PAGE showed an atypical migration profile, exhibiting many forms of different sizes and/or charge to mass ratio, with also possible oligomerization to form dimers (Fig. 7). Both chemical modifications of the enzyme were accompanied by a loss of its activity. These results suggest that oxidation or alkylation of reactive thiols could be modifying the tridimensional enzyme structure. These modifications include the formation of multiple monomeric forms (enzymatically inactive and having variable Stokes radii) that can interact between them giving rise to oligomers. This process seems also to occur *in vivo*, as found in *E. gracilis* cells grown under different axenic culture conditions in presence or absence of H_2O_2 (Fig. 8). Crude extract preparation of the microalgae was subjected to native PAGE or non-reducing SDS-PAGE, followed by electrotransference and western-blot to detect the native and denatured forms of *Egr*UDP-GlcPPase. As shown in

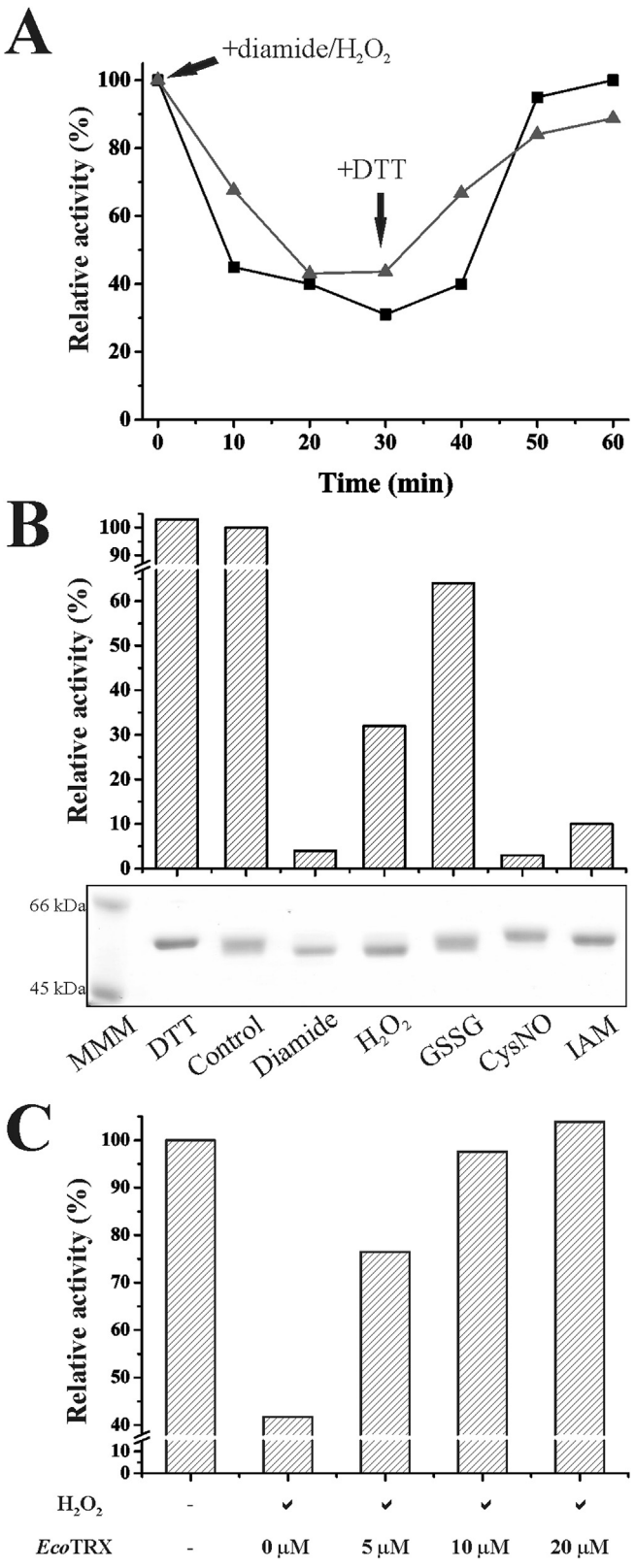

Fig. 5. A. *Egr*UDP-GlcPPase activity after oxidation and reduction by redox agents. The enzyme was tested during 30 min in the presence of diamide (■) or H_2O_2 (▲). The oxidized enzyme was then analyzed in the presence of dithiothreitol (DTT) during 30 min. **B.** UDP-GlcPPase relative activity and non-reducing SDS-PAGE of recombinant *Egr*UDP-GlcPPase incubated 30 min with a ratio of 200 [redox agent:enzyme] (both in μM). Molecular mass marker (MMM), dithiothreitol (DTT), no redox treatment (Control), hydrogen peroxide (H_2O_2), diamide, oxidized glutathione (GSSG), S-nitrosocysteine (CysNO) or iodoacetamide (IAM). **C.** Relative activity of the enzyme oxidized with H_2O_2 and subsequently reduced with different concentrations of reduced thioredoxin from *E. coli*. Hundred percent of activity (3350 U.mg^{-1}) corresponds the control that is the enzyme untreated with the oxidant.

Table 2
Thiols quantification of purified recombinant *Egr*UDP-GlcPPase. . Enzyme was incubated with different agents (agent:enzyme ratio of 5000 DTT, 500 diamide, 2000 H_2O_2 and 1000 IAM) during 30 min at 25 °C in buffer A.

Sample	Ratio [thiol/enzyme]
Control	6.3 ± 0.6
DTT	6.8 ± 0.8
Diamide	1.7 ± 0.3
H_2O_2	1.8 ± 0.3
IAM	2.4 ± 0.3

Fig. 8A, western-blots from native PAGE revealed a major protein band (with slight smear) in extracts from untreated cells (with relatively low oxidized status); whereas multiple forms and oligomeric interactions were found in samples from cells treated with H_2O_2 (under all growing conditions). Furthermore, western-blots from non-reducing SDS-PAGE revealed a single band under all conditions (Fig. 8B), suggesting that multiple forms observed for the oxidized enzyme are structures having different charge:mass ratio and lacking covalent intermolecular disulfide bonds. Fig. 8C shows the variation of the UDP-GlcPPase activity in crude extracts from cells grown axenically in different media and conditions, providing evidence for inactivation (associated to multiple molecular forms) in the presence of H_2O_2, mainly under autotrophic conditions.

4. Discussion

In the present study, a functional, catalytically active UDP-GlcPPase from *E. gracilis* has been biochemically characterized, and its cellular localization analyzed. A nucleotide sequence encoding a UTP-glucose-1-phosphate uridylyltransferase (*egrgalU*) was identified and *de novo* synthesized. The coded protein exhibited a high degree of identity with other protozoan UDP-GlcPPases as shown in an alignment with different homologous enzymes (supplemental Figure 1). The purified recombinant *Egr*UDP-GlcPPase was characterized in its kinetic properties. Besides the preferred substrates UTP and Glc-1P, the enzyme was able to use TTP, Gal-1P and Man-1P, with different catalytic efficiencies in synthesizing the respective sugar nucleotides: UDP-Glc ≫ TDP-Glc ≈ UDP-Gal > UDP-Man. By means of confocal microscopy and specific antibodies, the enzyme was visualized in the cytosol of *E. gracilis* cells, with a strong recognition signal in the flagellar region. Extracts from these cells exhibited relatively high levels of UDP-GlcPPase activity. Our findings are in agreement with previous reports on the metabolism of the protozoan, detecting high levels of glycosyl transferases in flagella [48]. In such a scenario, many of such glycosyl transferases use UDP-Glc as a substrate, justifying the presence of UDP-GlcPPase in the same cellular location. Moreover, recently O'Neill and co-workers [51] described UDP-Glc followed by TDP-Glc as the major nucleotide sugars present in this microorganism, coinciding with the presence of an active enzyme able to synthesize both metabolites.

In agreement with reports of the enzyme from other sources [41,52,53], active *Egr*UDP-GlcPPase was identified as a monomer and exhibited insensitivity to regulation by metabolites. Otherwise, both oxidants and alkylants exerted inactivation of the *E. gracilis* enzyme. The oxidized enzyme showed a recovery of the enzyme activity after reaction with reducing compounds (DTT and

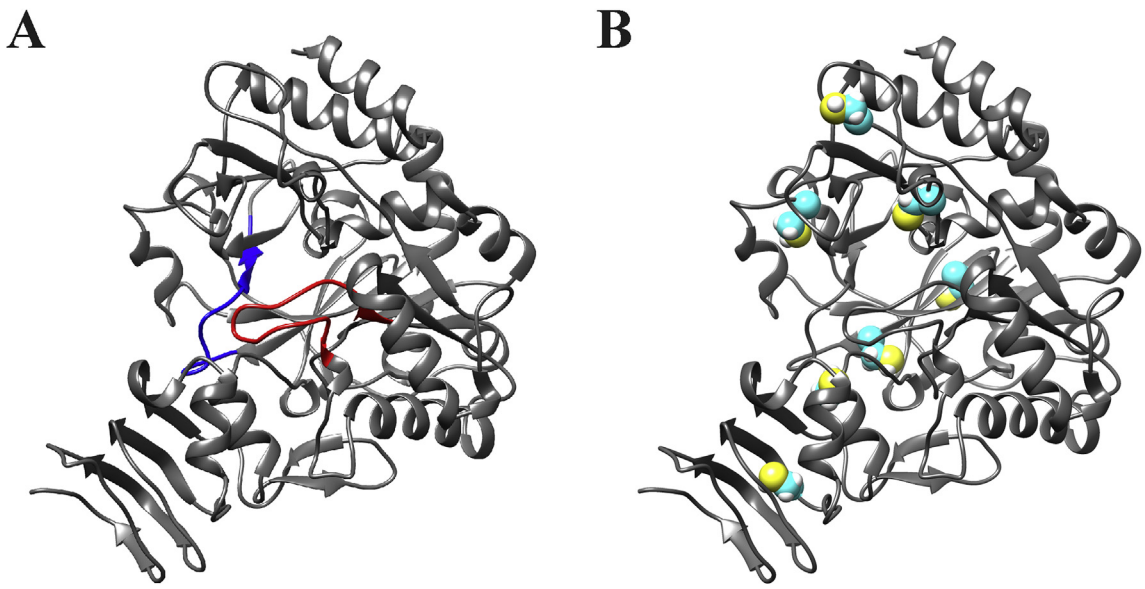

Fig. 6. Three dimensional model of *Egr*UDP-GlcPPase. The building of the structure model of *Egr*UDP-GlcPPase was based in a template derived from a known X-ray structure of the orthologous UDP-GlcPPase from *L. major* (PDB ID 4m2a, 54% identity) [32]. The global verify3D averaged a 3D-1D score of 90.63, indicating that our best model was in between the range of good predicted structures. Also, the stereochemical test reported 0.7% of residues in the disallowed area of Ramachandran plot [56] indicating that the backbone is folded in a reliable way. Moreover, the QMEAN value observed for this structure was −1.72, showing a good score for the evaluation performed by the structural descriptors used by this software [38]. **A.** Visualization of the amino acidic consensus for nucleotide (blue) and sugar (red) binding. **B.** The seven cysteine residues are shown as van der Waals spheres with the sulfur atoms are in yellow.

thioredoxins). This redox regulation has been reported to occur in the homologous enzymes from other protozoa [18,20], although the molecular mechanism by which Cys residues are oxidized has differences. In the UDP-Glc PPase from *E. histolytica* [20] and

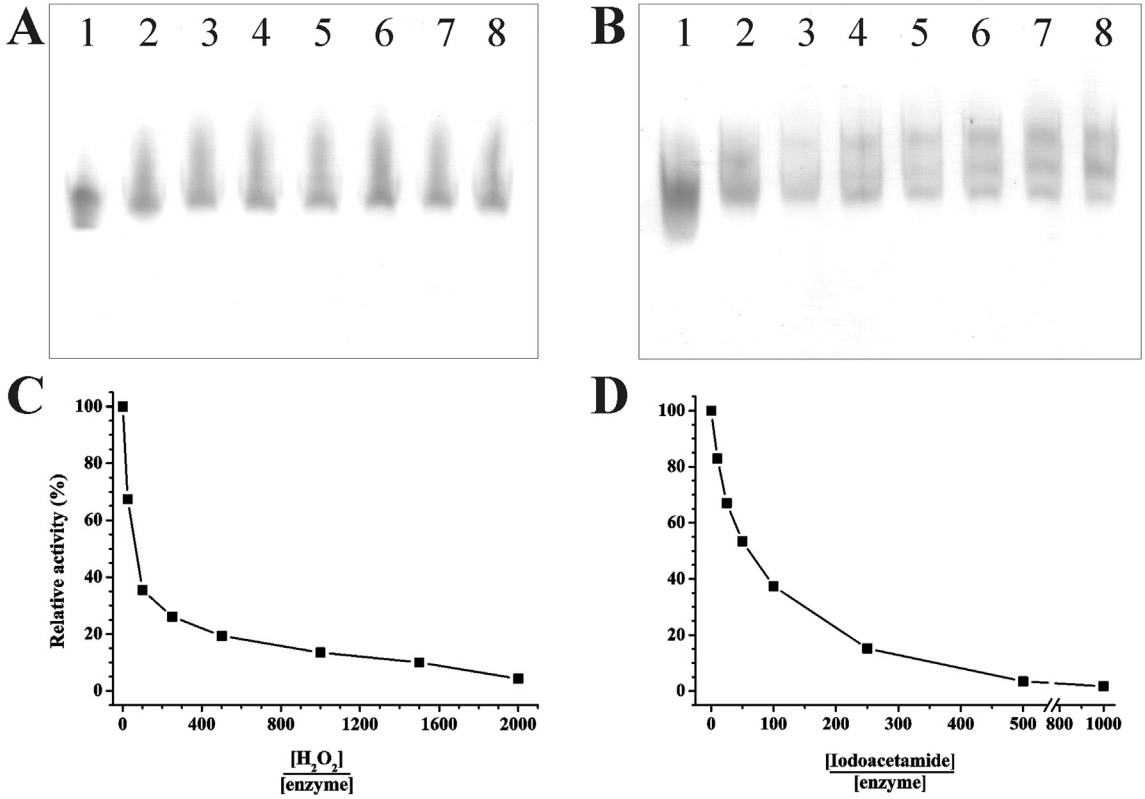

Fig. 7. Evaluation of purified recombinant *Egr*UDP-GlcPPase. **A.** native PAGE of the enzyme after incubation with increasing concentrations of H2O2. Ratio [H_2O_2]:[enzyme] (both in μM): 0, lane **1**; 25, lane **2**; 100, lane **3**; 250, lane **4**; 500, lane **5**; 1000, lane **6**; 1500, lane **7**; 2000, lane **8**. **B.** native PAGE of the enzyme incubated with IAM. Ratio [Iodoacetamide]:[enzyme] (both in μM): 0, lane **1**; 10, lane **2**; 25, lane **3**; 50, lane **4**; 100, lane **5**; 250, lane **6**; 500, lane **7**; 1000, lane **8**. **C.** Relative activity (%) of the respective samples from A. **D.** Relative activity (%) of the respective samples from B.

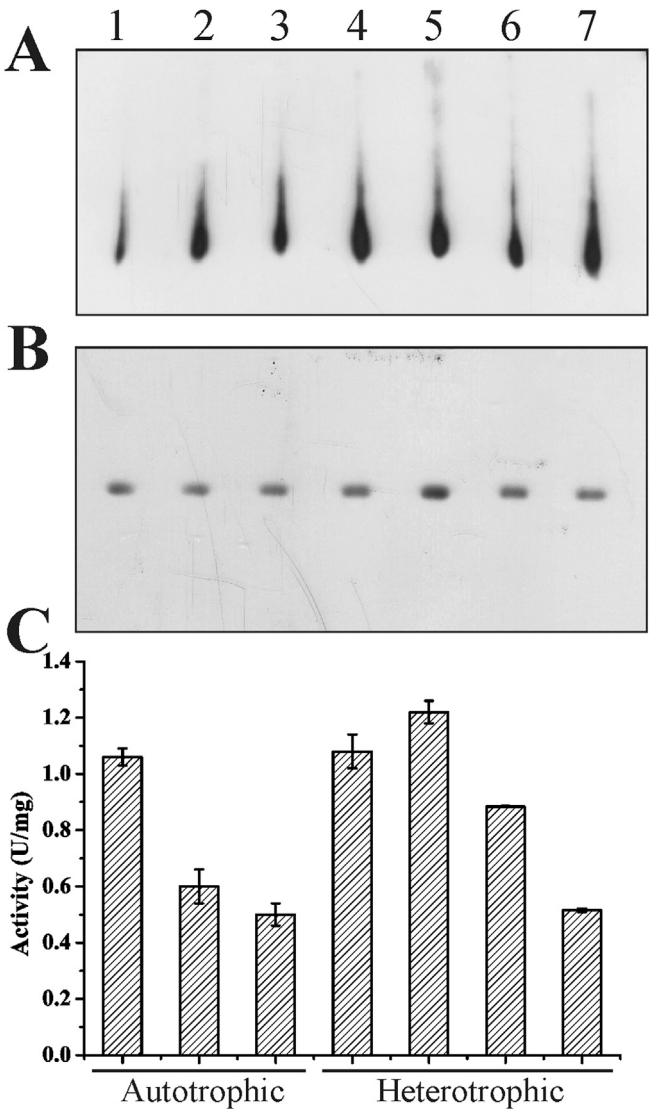

Fig. 8. Western-blot assays of **(A)** native PAGE; **(B)** non-reducing SDS-PAGE; and **(C)** UDP-GlcPPase activity from soluble fraction of *E. gracilis* cells. Lane **1,** autotrophic control cells (1.06 U.mg^{-1}); lane **2,** autotrophic cells treated with 250 μM H_2O_2 (0.6 U.mg^{-1}); lane **3,** autotrophic cells treated with 500 μM H_2O_2 (0.5 U.mg^{-1}); lane **4,** heterotrophic control cells (1.08 U.mg^{-1}); lane **5,** heterotrophic cells treated with 250 μM H_2O_2 (1.22 U.mg^{-1}); lane **6,** heterotrophic cells in anaerobiosis conditions (C&M medium supplemented with 1% Glc) (0.88 U.mg^{-1}); lane **7,** heterotrophic cells in anaerobiosis conditions (C&M medium without carbon source) (0.52 U.mg^{-1}).

G. lamblia [18], inactivation by H_2O_2 involves the formation of an intrasubunit disulfide bond between Cys108 and Cys378 (numbers as in the *E. histolytica* protein), residues that are close to each other in the 3-D structure, and involved in a critical nucleotide binding site together with Met106. In contrast, in the 3D-structure of *Egr*UDP-GlcPPase none of the seven Cys residues would be close enough each other to form intra or inter subunit disulfides. The latter has a Cys residue aligning with Cys 378 but lacks the equivalent Cys108 of the *E. histolytica* protein (supplemental Figure 1). For the *E. gracilis* enzyme the mechanism of redox inactivation involves alkylation or oxidation (to sulfenic acid derivatives) of five Cys. This provokes the formation of multiple protein structures having different Stokes radii; which, in turn, could form oligomers by non-covalent interactions. Concerning these changes in protein structures and oligomerization, it is worth considering that the UDP-GlcPPase from barley was found to be regulated by oligomerization, with the formation of inactive dimeric and trimeric structures under certain environmental conditions (depending on the buffer used, the protein dilution and the presence of orthophosphate) [52,53]. Although oligomerization of the plant enzyme has no direct relation with redox modification, it was found that DTT is effective for deoligomerization with recovery of enzyme activity [52].

Results presented here suggest that the particular mechanism by which *Egr*UDP-GlcPPase is modified in activity and structure by redox compounds is operative *in vivo*. In this respect, we detected single (highly active) or multiple forms (with lower activity) of the enzyme in extracts from *E. gracilis* cells grown under normal or oxidative stress conditions, respectively. These results were in very good agreement with the characterization of redox modulation performed by studies *in vitro* with the recombinant purified enzyme, including the complete reversion (in enzyme activity as well as in protein structure) of the effect of redox oxidants reached by treatment with reductants. The whole set of data, together with the fact that many of the redox effectors (H_2O_2, GSSG, thioredoxin) are molecules present in cells strongly suggests that in *E. gracilis* UDP-GlcPPase is reversibly regulated by redox chemical modification. This regulation involves not only the modulation of the enzyme activity but also changes it the protein structure. Consistent with this, it is tempting to speculate that *Egr*UDP-GlcPPase could be considered as a moonlighting enzyme [54,55]. A moonlighting protein performs multiple (physiologically relevant) functions, which in some cases are switched by chemical modification. In the case of *Egr*UDP-GlcPPase, oxidation by redox compounds would trigger conformational changes and oligomerization of the protein with change in its function from being an enzyme involved in carbohydrates metabolism to any other one(s). Elucidation of novel function(s) for this enzyme remains an open question and further work is necessary to reinforce the moonlighting characteristic of the protein in euglenoids.

5. Conclusions

E. gracilis, a unicellular protozoa feeding both by photosynthesis and heterotrophically, uses UDP-glucose as substrate for paramylon synthesis and for carbohydrate metabolism. The gene coding for a putative UDP-GlcPPase was cloned and the enzyme produced recombinantly to high purity. The presence of the enzyme in cytosol and flagellar space was demonstrated *in vivo*. The enzymatic characterization of the enzyme supports its ability to catalyze synthesis of UDP-Glc, TDP-Glc, UDP-Gal and UDP-Man. We identified redox modification of the enzyme producing conformational changes and giving different protein structures (monomers with different Stokes radii that interact forming oligomers) with loss of activity. Thus, the *Egr*UDP-GlcPPase activity could be redox modulated *in vivo*.

Acknowledgments

We thank to Dr Ellis O'Neill and Dr. Robert Field, from the Biological Chemistry Department at the John Innes Centre in United Kingdoms, for kindly share information about transcriptomics and genomics of *E. gracilis*. We acknowledge Dr. Hannah N. Sivak for English proof-reading and advice. RJM and RDC are doctoral fellowship from CONICET and ANPCyT respectively. DGA, FEH and SAG are investigator career members from CONICET. This work was supported by grants from CONICET (PIO-YPF), ANPCyT (PICT 2014-2103, PICT 2015-1149, PICT 2015-1767, PICT 2016-1110) and UNL (CAID 2016).

Appendix A. Supplementary data

Supplementary data to this article can be found online at https://doi.org/10.1016/j.biochi.2018.09.006.

References

[1] M. Rogers, P.J. Keeling, Lateral transfer and recompartmentalization of Calvin cycle enzymes of plants and algae, J. Mol. Evol. 58 (2004) 367–375.
[2] E. Suzuki, R. Suzuki, Variation of storage polysaccharides in phototrophic microorganisms, J. Appl. Glycosci. 60 (2013) 21–27.
[3] E.V. Armbrust, J.A. Berges, C. Bowler, B.R. Green, D. Martinez, N.H. Putnam, S. Zhou, A.E. Allen, K.E. Apt, M. Bechner, M.A. Brzezinski, B.K. Chaal, A. Chiovitti, A.K. Davis, M.S. Demarest, J.C. Detter, T. Glavina, D. Goodstein, M.Z. Hadi, U. Hellsten, M. Hildebrand, B.D. Jenkins, J. Jurka, V.V. Kapitonov, N. Kroger, W.W. Lau, T.W. Lane, F.W. Larimer, J.C. Lippmeier, S. Lucas, M. Medina, A. Montsant, M. Obornik, M.S. Parker, B. Palenik, G.J. Pazour, P.M. Richardson, T.A. Rynearson, M.A. Saito, D.C. Schwartz, K. Thamatrakoln, K. Valentin, A. Vardi, F.P. Wilkerson, D.S. Rokhsar, The genome of the diatom Thalassiosira pseudonana: ecology, evolution, and metabolism, Science 306 (2004) 79–86.
[4] S.A. Breglia, N. Yubuki, M. Hoppenrath, B.S. Leander, Ultrastructure and molecular phylogenetic position of a novel euglenozoan with extrusive episymbiotic bacteria: bihospites bacati n. gen. et sp. (Symbiontida), BMC Microbiol. 10 (2010) 145.
[5] N. Yubuki, V.P. Edgcomb, J.M. Bernhard, B.S. Leander, Ultrastructure and molecular phylogeny of Calkinsia aureus: cellular identity of a novel clade of deep-sea euglenozoans with epibiotic bacteria, BMC Microbiol. 9 (2009) 16.
[6] L. Bonen, Trans-splicing of pre-mRNA in plants, animals, and protists, Faseb. J. 7 (1993) 40–46.
[7] X.H. Liang, A. Haritan, S. Uliel, S. Michaeli, Trans and cis splicing in trypanosomatids: mechanism, factors, and regulation, Eukaryot. Cell 2 (2003) 830–840.
[8] A.G. Simpson, Cytoskeletal organization, phylogenetic affinities and systematics in the contentious taxon Excavata (Eukaryota), Int. J. Syst. Evol. Microbiol. 53 (2003) 1759–1777.
[9] N. Yubuki, A.G. Simpson, B.S. Leander, Comprehensive ultrastructure of Kipferlia bialata provides evidence for character evolution within the Fornicata (Excavata), Protist 164 (2013) 423–439.
[10] D. Gerbod, E. Sanders, S. Moriya, C. Noel, H. Takasu, N.M. Fast, P. Delgado-Viscogliosi, M. Ohkuma, T. Kudo, M. Capron, J.D. Palmer, P.J. Keeling, E. Viscogliosi, Molecular phylogenies of Parabasalia inferred from four protein genes and comparison with rRNA trees, Mol. Phylogenet. Evol. 31 (2004) 572–580.
[11] V. Hampl, L. Hug, J.W. Leigh, J.B. Dacks, B.F. Lang, A.G. Simpson, A.J. Roger, Phylogenomic analyses support the monophyly of Excavata and resolve relationships among eukaryotic "supergroups", Proc. Natl. Acad. Sci. U. S. A. 106 (2009) 3859–3864.
[12] E.C. O'Neill, M. Trick, L. Hill, M. Rejzek, R.G. Dusi, C.J. Hamilton, P.V. Zimba, B. Henrissat, R.A. Field, The transcriptome of Euglena gracilis reveals unexpected metabolic capabilities for carbohydrate and natural product biochemistry, Mol. Biosyst. 11 (2015) 2808–2820.
[13] Y. Yoshida, T. Tomiyama, T. Maruta, M. Tomita, T. Ishikawa, K. Arakawa, De novo assembly and comparative transcriptome analysis of Euglena gracilis in response to anaerobic conditions, BMC Genom. 17 (2016) 182.
[14] J. Briand, R. Calvayrac, D. Laval-Martin, J. Farineau, Evolution of carboxylating enzymes involved in paramylon synthesis (phosphoenolpyruvate carboxylase and carboxykinase) in heterotrophically grown Euglena gracilis, Planta 151 (1981) 168–175.
[15] A.E. Clarke, B.A. Stone, Structure of the paramylon from Euglena gracilis, Biochim. Biophys. Acta 44 (1960) 161–163.
[16] S.H. Goldemberg, L.R. Marechal, Biosynthesis of paramylon in Euglena gracilis, Biochim. Biophys. Acta 71 (1963) 743–744.
[17] P. Teerawanichpan, X. Qiu, Fatty acyl-CoA reductase and wax synthase from Euglena gracilis in the biosynthesis of medium-chain wax esters, Lipids 45 (2010) 263–273.
[18] A.C. Ebrecht, M.D. Asencion Diez, C.V. Piattoni, S.A. Guerrero, A.A. Iglesias, The UDP-glucose pyrophosphorylase from Giardia lamblia is redox regulated and exhibits promiscuity to use galactose-1-phosphate, Biochim. Biophys. Acta 1850 (2015) 88–96.
[19] K. Marino, M.L. Guther, A.K. Wernimont, M. Amani, R. Hui, M.A. Ferguson, Identification, subcellular localization, biochemical properties, and high-resolution crystal structure of Trypanosoma brucei UDP-glucose pyrophosphorylase, Glycobiology 20 (2010) 1619–1630.
[20] L.I. Martinez, C.V. Piattoni, S.A. Garay, D.E. Rodrigues, S.A. Guerrero, A.A. Iglesias, Redox regulation of UDP-glucose pyrophosphorylase from Entamoeba histolytica, Biochimie 93 (2011) 260–268.
[21] T. Yang, M. Bar-Peled, Identification of a novel UDP-sugar pyrophosphorylase with a broad substrate specificity in Trypanosoma cruzi, Biochem. J. 429 (2010) 533–543.
[22] J. Sambrook, D.W. Russell, Molecular Cloning: a Laboratory Manual. Third, Cold pring Harbor Laboratory Press, New York, 2001.
[23] M. Cramer, J. Myers, Growth and photosynthetic characteristics of Euglena gracilis, Arch. Mikrobiol. 17 (1952) 384–402.
[24] M.M. Bradford, A rapid and sensitive method for the quantitation of microgram quantities of protein utilizing the principle of protein-dye binding, Anal. Biochem. 72 (1976) 248–254.
[25] U.K. Laemmli, Cleavage of structural proteins during the assembly of the head of bacteriophage T4, Nature 227 (1970) 680–685.
[26] C. Arndt, S. Koristka, H. Bartsch, M. Bachmann, Native Polyacrylamide Gels, Protein Electrophoresis, Springer, 2012, pp. 49–53.
[27] J.L. Vaitukaitis, Production of antisera with small doses of immunogen: multiple intradermal injections, Methods Enzymol. 73 (1981) 46–52.
[28] D.G. Arias, V.E. Marquez, M.L. Chiribao, F.R. Gadelha, C. Robello, A.A. Iglesias, S.A. Guerrero, Redox metabolism in Trypanosoma cruzi: functional characterization of tryparedoxins revisited, Free Radical Biol. Med. 63 (2013) 65–77.
[29] D.G. Arias, A. Reinoso, N. Sasoni, M.D. Hartman, A.A. Iglesias, S.A. Guerrero, Kinetic and structural characterization of a typical two-cysteine peroxiredoxin from Leptospira interrogans exhibiting redox sensitivity, Free Radical Biol. Med. 77 (2014) 30–40.
[30] C. Fusari, A.M. Demonte, C.M. Figueroa, M. Aleanzi, A.A. Iglesias, A colorimetric method for the assay of ADP-glucose pyrophosphorylase, Anal. Biochem. 352 (2006) 145–147.
[31] M. Biasini, S. Bienert, A. Waterhouse, K. Arnold, G. Studer, T. Schmidt, F. Kiefer, T. Gallo Cassarino, M. Bertoni, L. Bordoli, T. Schwede, SWISS-MODEL: modelling protein tertiary and quaternary structure using evolutionary information, Nucleic Acids Res. 42 (2014) W252–W258.
[32] J. Führing, J.T. Cramer, F.o.H. Routier, A.-C. Lamerz, P. Baruch, R. Gerardy-Schahn, R. Fedorov, Catalytic mechanism and allosteric regulation of UDP-glucose pyrophosphorylase from Leishmania major, ACS Catal. 3 (2013) 2976–2985.
[33] M. Remmert, A. Biegert, A. Hauser, J. Soding, HHblits: lightning-fast iterative protein sequence searching by HMM-HMM alignment, Nat. Methods 9 (2011) 173–175.
[34] B. Webb, A. Sali, Comparative protein structure modeling using MODELLER, Curr Protoc Bioinformatics 47 (2014) 5 6 1–32.
[35] B. Webb, A. Sali, Protein structure modeling with MODELLER, Meth. Mol. Biol. 1137 (2014) 1–15.
[36] D. Eisenberg, R. Luthy, J.U. Bowie, VERIFY3D: assessment of protein models with three-dimensional profiles, Methods Enzymol. 277 (1997) 396–404.
[37] M.Y. Shen, A. Sali, Statistical potential for assessment and prediction of protein structures, Protein Sci. 15 (2006) 2507–2524.
[38] P. Benkert, M. Kunzli, T. Schwede, QMEAN server for protein model quality estimation, Nucleic Acids Res. 37 (2009) W510–W514.
[39] D.G. Yi, W.K. Huh, UDP-glucose pyrophosphorylase Ugp1 is involved in oxidative stress response and long-term survival during stationary phase in Saccharomyces cerevisiae, Biochem. Biophys. Res. Commun. 467 (2015) 657–663.
[40] Q. Yu, X. Zheng, The crystal structure of human UDP-glucose pyrophosphorylase reveals a latch effect that influences enzymatic activity, Biochem. J. 442 (2012) 283–291.
[41] A.C. Lamerz, T. Haselhorst, A.K. Bergfeld, M. von Itzstein, R. Gerardy-Schahn, Molecular cloning of the Leishmania major UDP-glucose pyrophosphorylase, functional characterization, and ligand binding analyses using NMR spectroscopy, J. Biol. Chem. 281 (2006) 16314–16322.
[42] M.B. Bosco, M. Machtey, A.A. Iglesias, M. Aleanzi, UDPglucose pyrophosphorylase from Xanthomonas spp. Characterization of the enzyme kinetics, structure and inactivation related to oligomeric dissociation, Biochimie 91 (2009) 204–213.
[43] F.S. Fernandez, S.E. Trombetta, U. Hellman, A.J. Parodi, Purification to homogeneity of UDP-glucose:glycoprotein glucosyltransferase from Schizosaccharomyces pombe and apparent absence of the enzyme fro Saccharomyces cerevisiae, J. Biol. Chem. 269 (1994) 30701–30706.
[44] C.M. Figueroa, M.D. Asencion Diez, M.L. Kuhn, S. McEwen, G.L. Salerno, A.A. Iglesias, M.A. Ballicora, The unique nucleotide specificity of the sucrose synthase from Thermosynechococcus elongatus, FEBS Lett. 587 (2013) 165–169.
[45] M.A. Ballicora, A.A. Iglesias, J. Preiss, ADP-glucose pyrophosphorylase, a regulatory enzyme for bacterial glycogen synthesis, Microbiol. Mol. Biol. Rev. 67 (2003) 213–225, table of contents.
[46] A.A. Iglesias, J. Preiss, Bacterial glycogen and plant starch biosynthesis, Biochem. Mol. Biol. Educ. 20 (1992) 196–203.
[47] J.B. Schenkman, D.L. Cinti, Preparation of Microsomes with Calcium, Methods Enzymol, Elsevier, 1978, pp. 83–89.
[48] S.J. Chen, G.B. Bouck, Endogenous glycosyltransferases glucosylate lipids in flagella of Euglena, J. Cell Biol. 98 (1984) 1825–1835.
[49] P. Eyer, F. Worek, D. Kiderlen, G. Sinko, A. Stuglin, V. Simeon-Rudolf, E. Reiner, Molar absorption coefficients for the reduced Ellman reagent: reassessment, Anal. Biochem. 312 (2003) 224–227.
[50] L.B. Poole, Formation and Functions of Protein Sulfenic Acids, Current Protocols in Toxicology (Chapter 17), 2004. Unit17 11.
[51] E.C. O'Neill, S. Kuhaudomlarp, M. Rejzek, J.U. Fangel, K. Alagesan, D. Kolarich, W.G.T. Willats, R.A. Field, Exploring the glycans of euglena gracilis, Biology 6 (2017).

[52] L.A. Kleczkowski, F. Martz, M. Wilczynska, Factors affecting oligomerization status of UDP-glucose pyrophosphorylase, Phytochemistry 66 (2005) 2815–2821.
[53] M. Meng, E. Fitzek, A. Gajowniczek, M. Wilczynska, L.A. Kleczkowski, Domain-specific determinants of catalysis/substrate binding and the oligomerization status of barley UDP-glucose pyrophosphorylase, Biochim. Biophys. Acta 1794 (2009) 1734–1742.
[54] D.H. Huberts, I.J. van der Klei, Moonlighting proteins: an intriguing mode of multitasking, Biochim. Biophys. Acta 1803 (2010) 520–525.
[55] C.J. Jeffery, Protein species and moonlighting proteins: very small changes in a protein's covalent structure can change its biochemical function, Journal of proteomics 134 (2016) 19–24.
[56] G.N. Ramachandran, C. Ramakrishnan, V. Sasisekharan, Stereochemistry of polypeptide chain configurations, J. Mol. Biol. 7 (1963) 95–99.